Received: 3 August 2020 | Revised: 24 February 2021 | Accepted: 1 March 2021

DOI: 10.1111/mec.15874

ORIGINAL ARTICLE

MOLECULAR ECOLOGY WILEY

Pheromone receptor of the globally invasive quarantine pest of the palm tree, the red palm weevil (*Rhynchophorus ferrugineus*)

Binu Antony[1] | Jibin Johny[1] | Nicolas Montagné[2] | Emmanuelle Jacquin-Joly[2] | Rémi Capoduro[2] | Khasim Cali[3] | Krishna Persaud[3] | Mohammed Ali Al-Saleh[1] | Arnab Pain[4]

[1]Department of Plant Protection, College of Food and Agricultural Sciences, Center for Chemical Ecology and Functional Genomics, Chair of Date Palm Research, King Saud University, Riyadh, Saudi Arabia

[2]INRAE, Sorbonne Université, CNRS, IRD, UPEC, Institute of Ecology and Environmental Sciences of Paris, iEES-Paris, Université Paris Diderot, Versailles, France

[3]Department of Chemical Engineering and Analytical Science, The University of Manchester, Manchester, UK

[4]BESE Division, King Abdullah University of Science and Technology (KAUST), Jeddah, Saudi Arabia

Correspondence
Binu Antony, Department of Plant Protection, Center for Chemical Ecology and Functional Genomics, College of Food and Agricultural Sciences, Chair of Date Palm Research, King Saud University, Riyadh 11451, Saudi Arabia.
Email: bantony@ksu.edu.sa

Funding information
King Abdulaziz City for Science and Technology, Grant/Award Number: KACST-NSTIP-12-AGR-2854-02; King Abdullah University of Science and Technology, Grant/Award Number: KAUST-OSR-2018-RPW-3816; ANR Investissements d'avenir program "PheroSensor" of France

Abstract

Palm trees are of immense economic, sociocultural, touristic, and patrimonial significance all over the world, and date palm-related knowledge, traditions, and practices are now included in UNESCOs list of the Intangible Cultural Heritage of Humanity. Of all the pests that infest these trees, the red palm weevil (RPW), *Rhynchophorus ferrugineus* (Olivier), is its primary enemy. The RPW is a category-1 quarantine insect pest that causes enormous economic losses in palm tree cultivation worldwide. The RPW synchronizes mass gathering on the palm tree for feeding and mating, regulated by a male-produced pheromone composed of two methyl-branched compounds, (4*RS*, 5*RS*)-4-methylnonan-5-ol (ferrugineol) and 4(*RS*)-methylnonan-5-one (ferrugineone). Despite the importance of odorant detection in long-range orientation towards palm trees, palm colonization, and mating, the pheromone receptor has not been identified in this species. In this study, we report the identification and characterization of the first RPW pheromone receptor, *RferOR1*. Using gene silencing and functional expression in *Drosophila* olfactory receptor neurons, we demonstrate that *RferOR1* is tuned to ferrugineol and ferrugineone and binds five other structurally related molecules. We reveal the lifetime expression of *RferOR1*, which correlates with adult mating success irrespective of age, a factor that could explain the wide distribution and spread of this pest. As palm weevils are challenging to control based on conventional methods, elucidation of the mechanisms of pheromone detection opens new routes for mating disruption and the early detection of this pest via the development of pheromone receptor-based biosensors.

KEYWORDS
aggregation pheromone, deorphanization, pheromone receptor, red palm weevil, *Rhynchophorus ferrugineus*

1 | INTRODUCTION

The red palm weevil (RPW), *Rhynchophorus ferrugineus*, is the most damaging insect pest of palm trees and responsible for massive economic losses worldwide. Originating from South Asia, this invasive weevil has spread through the Middle East, Africa and the whole Mediterranean area since 1980. Its control relies mainly on the use of systemic insecticides, but ecofriendly management techniques, such as the inclusion of pheromone traps in integrated pest management strategies, have emerged. Pheromone traps are also used

to monitor populations and new potential invasions, as this species poses a global threat.

The RPW pheromone is composed of two methyl-branched short-chain hydrocarbons, (4*RS*,5*RS*)-4-methylnonan-5-ol (ferrugineol) and (4*RS*,5*RS*)-4-methylnonan-5-one (ferrugineone), at a 9:1 ratio. It is produced by males and leads to coordinated mass attacks that often cause the collapse and death of the palm tree (Oehlschlager, 2016). Despite the fundamental importance of this pheromone in RPW mass attack and sexual reproduction as well as its use for insect control, nothing regarding the mechanisms of its recognition by these insects is known. It is hypothesized that this airborne pheromone is detected by a specific subclass of odorant receptors (ORs) specialized in pheromone detection. Indeed, most odorants are detected in insects via the activation of ORs, which act as gate-keepers of selectivity and sensitivity (Breer et al., 2019; Meinwald et al., 2018). These ORs are heptahelical transmembrane proteins embedded in the dendritic membrane of olfactory receptor neurons (ORNs) housed in olfactory sensilla on the antennae. Compared to G-protein-coupled receptors (GPCRs), insect ORs present an inverse topology, N_{in}–C_{out}, and insect ORs function as ligand-gated nonselective cation channels (Benton et al., 2006; Butterwick et al., 2018) via heteromeric complexes formed by an odorant-specific OR protein and a highly conserved coreceptor (Orco) (Larsson et al., 2004; Leal, 2013; Sato et al., 2008; Vosshall & Hansson, 2011; Wicher et al., 2008). Encoded messages are conveyed to the central nervous system in the antennal lobe, where the neural signal is decoded (Fleischer et al., 2018; Leal, 2013). Thus, insect ORs are the main gateway to sensing the world of volatile chemicals (Leal, 2013, 2014; Meinwald et al., 2018). Although many OR sequences from a range of insect species, including that of the RPW (Antony et al., 2016), are now available, information about the functional role of ORs remains limited to the OR repertoires of a few model organisms, such as the fruit fly *Drosophila melanogaster* (Mansourian & Stensmyr, 2015), and ORs tuned to particular signals, such as moth sex pheromones (Breer et al., 2019; Fleischer et al., 2018; Montagné et al., 2015; Nakagawa et al., 2005). Notably, the response spectra of only a handful of ORs have been studied in beetles (Coleoptera) (Mitchell et al., 2012; Yuvaraj et al., 2021), even though they constitute the most species-rich insect order. In particular, no RPW ORs have been functionally characterized. In this study, we specifically screened for RPW aggregation pheromone receptors by selectively silencing ORs highly expressed in the antennae using RNA interference and assessing changes in pheromone detection using electrophysiological recordings. By doing so, we identified one OR, *RferOR1*, as the best candidate pheromone receptor. We then heterologously expressed it in *Drosophila* ORNs and established its response spectrum to a large panel of weevil and palm beetle pheromone components. *RferOR1* was best activated by ferrugineol and ferrugineone and slightly less activated by five other structurally related molecules, thus demonstrating its functional role as a *R. ferrugineus* aggregation pheromone receptor. Subsequently, we modelled the three-dimensional structure of *RferOR1* and proposed binding sites.

This work represents an essential step in our understanding of RPW bioecology. This study identifies an OR as a new target for the development of pheromone receptor-based biosensors for the early detection of RPWs in the field.

2 | MATERIALS AND METHODS

2.1 | Palm weevil field collection, rearing, and tissue collection

The original collections of *R. ferrugineus* were made from date palm orchards of the Al-Kharj region (24.1500° N, 47.3000° E) of Saudi Arabia in the year 2009. Since then, the culture was maintained in our laboratory on sugarcane stems, as previously described (Abdel-Azim et al., 2012). This RPW culture is further referred to as the laboratory-reared population, used for the OR expression analysis, pheromone pre-exposure experiment, and gene silencing through RNA interference (RNAi) studies. Two field RPW populations were collected from two different date palm orchards where high infestations have been reported in the Al Qassim (25.8275° N, 42.8638° E) and Al Kharj (24.1500° N, 47.3000° E) regions during April–May 2017. These two field populations are further referred to as field-collected RPWs (Fld1 and Fld2), specifically used to compare OR expression in the pheromone pre-exposure experiments. The adult male and female antennal dissections and different tissue collections were performed after insects were anaesthetized using CO_2 for 1–2 min, as described in the Methods S1.

2.2 | *RferOR* phylogenetic analysis, expression analyses and pheromone pre-exposure experiments

Phylogenetic analysis was performed using previously annotated OR amino acid sequences from *R. ferrugineus* (Antony et al., 2016), *Ips typographus* (Yuvaraj et al., 2021), *Megacyllene caryae* (Mitchell et al., 2012), *Dendroctonus ponderosae* (Andersson et al., 2019) and *Nicrophorus vespilloides* (Mitchell et al., 2020) to identify gene orthologues and paralogues. Multiple sequence alignments were performed using MAFFT v.7 (Katoh et al., 2017), with the E-INS-i iterative refinement strategy and default parameters, followed by manual trimming. The JTT+G + F substitution model was determined as the best-fit model of protein evolution based on the AIC by using ProtTest *v.* 3.4 (Darriba et al., 2011). Phylogenetic reconstruction and analysis of the OR distribution were performed via the maximum likelihood method with 100 bootstrap replications using RAxML *v.* 8 (Stamatakis, 2014).

The expression of 71 *RferORs* previously identified in the antennal transcriptome (Antony et al., 2016) was mapped in the male and female antennae and male snout, legs, thorax, abdomen, and

wings of 20-day-old adult insects using RT-PCR (Methods S1). Expression of the 20 antennae-specific *RferORs* in the male and female antennae of individuals from the laboratory colony and two date palm field populations was quantified using RT-qPCR. We selected 20-day-old adults for the *RferOR* expression analysis based on a recent report of higher *RferOrco* expression at this age (Soffan et al., 2016). RT-qPCR assays were performed in the Applied Biosystems 7500 Fast Real-Time PCR Systems (SYBR Green PCR Master Mix, Thermo Fisher) using the thermal program mentioned in the Methods S1. Relative expression levels of *RferOR* genes were measured by normalization to tubulin and β-actin (Antony et al., 2018) (Table S1).

Pheromone pre-exposure experiments were conducted on laboratory-reared RPW adults to test whether this exposure would affect the expression levels of the 20 antennae-specific *RferORs*. Male and female adults were isolated in separate stimulus containers and were pre-exposed to a synthetic pheromone blend (ChemTica Int., Costa Rica) composed of ferrugineol and ferrugineone (9:1) during 4 h (see details in Methods S1). The adults were immediately killed by immersion in liquid nitrogen, and the antennae were dissected, and the total RNA was extracted (Methods S1). The relative expression analysis of the 20 antennal-specific *RferORs* was performed using RT-qPCR, and relative expression levels were compared with those in field-collected RPWs. Laboratory-reared RPWs that were not exposed to pheromone stimuli were used as a negative control. Changes in *RferOR* expression in response to exposure to pheromone were calculated using the $2^{-\Delta\Delta Ct}$ method (Schmittgen & Livak, 2008) by normalizing them to tubulin and β-actin and using the negative control (laboratory reared RPWs) as reference. More detailed descriptions are available in Methods S1.

2.3 | Gene silencing and RT-qPCR validation

The full-length open reading frame sequences of the six most highly expressed *RferORs* were obtained by amplifying both the "5" and "3" cDNA ends using the rapid amplification of cDNA ends technique (Antony et al., 2018; Soffan et al., 2016) (Methods S1). Full-length double-stranded RNAs (dsRNAs) were synthesized through in vitro transcription using the MEGAscript RNAi Kit (Life Technologies) following a previously described method (Antony et al., 2018, 2019; Soffan et al., 2016). The dsRNA-injected RPW pupae were maintained on sugarcane stems in a rearing room (Methods S1), as previously described (Soffan et al., 2016). Nine lines of injected weevils were generated: six lines that were each injected with one of the OR dsRNAs and three control lines. Controls consisted of weevils injected with a universal negative dsRNA control (Integrated DNA Technologies) (hereafter, negative control), weevils that were not injected (hereafter, NI), and weevils injected with nuclease-free water (hereafter, NFW). The emerging adults were transferred to a separate box containing a piece of fresh sugarcane and maintained for 21 days until their use in behavioural assays and electrophysiology experiments (see details in Methods S1). For RT-qPCR verification of transcript knockdown, the antennae of 21-day-old adult weevils were separately dissected, and qPCR was conducted using the methods described above (Antony et al., 2018). The relative expression levels of *RferORs* were measured with the $2^{-\Delta\Delta Ct}$ method by normalizing them to tubulin and β-actin and using the dsRNA negative control as reference. The significant changes in expression were estimated by one-way ANOVA, followed by multiple-comparison testing with the least significant difference (LSD) test using SPSS *v*24 (IBM SPSS statistics).

2.4 | Olfactometer assay and electroantennography (EAG)

We followed previously described methods (Antony et al., 2018; Soffan et al., 2016). Briefly, for behavioural studies, 15- to 18-day-old adult insects from the nine lines of aforementioned injected weevils were starved overnight (approximately 8 h), and the response of each insect to pheromone stimulation was recorded in a Y-tube olfactometer (Volatile Collection System Co.). Each experimental group (*RferOR* dsRNA-injected, dsRNA negative control, and NFW-injected) consisted of eight male and eight female adults. Each RPW adult was used three times on different days; in addition, recordings were performed randomly by shifting the dsRNA and NI RPW adults and changing the Y-branch olfactometer's orientations. Usually, the RPW adults were able to locate the pheromone stimulus within 2–3 min. A run was terminated if the weevil failed to move beyond the first 3 cm of the main tube within 5 min of release, and they were recorded as "no response" (Soffan et al., 2016). The choice of individual insects ("stimulus", "air", or "no response") was recorded three times on different days, and results were represented as percentages. A one-way ANOVA and LSD method was used to test significant differences among different experimental groups, followed by the Waller-Duncan multiple comparison test (SPSS) to determine the homogenous subset.

To confirm the *RferOR* knockdown effect on RPW adults, the same individuals used in the olfactometer assay were tested for their antennal response to the pheromone using EAG (Syntech). For EAG experiments, six 21-day-old adult RPWs were tested per experimental group (*RferOR* dsRNA-injected, NFW-injected, and NI). The antennal responses (EAG) to each stimulus – ferrugineol, ferrugineone, and ethyl acetate (diluted in *n*-hexane and 200 ng loaded in the stimulus cartridge) were recorded, with charcoal-filtered humidified air used as a negative control, using a Syntech Acquisition IDAC-2 controller connected to a computer and processed using EAG 2012 v1.2.4 (Syntech). More detailed descriptions are available in Methods S1. For each insect, the EAG amplitude measured in response to clean air (negative control) was subtracted from the EAG amplitude in response to the stimulus prior to statistical analysis (Olsson & Hansson, 2013). Significant differences in EAG responses among the different experimental groups were analysed by one-way ANOVA, followed by a Tukey's honest significant difference (HSD) test (SPSS).

2.5 | Transgenic expression of *RferOR1* in *Drosophila* ORNs

The ORF encoding *RferOR1* was cloned into the pUAST.attB vector (Methods S1) (Table S1). Transgenic *D. melanogaster UAS-RferOR1* lines were generated by BestGene Inc. by injecting the EndoFree *pUAST.attB-RferOR1* plasmid into fly embryos expressing the integrase PhiC31 and carrying an *attP* landing site within region ZH-51C of the second chromosome (Bischof et al., 2007). *Drosophila* lines expressing the *RferOR1* transgene in at1 trichoid sensillum ORNs (genotype *w*; *UAS-RferOR1*,w^+; $Or67d^{GAL4}$) were generated by crossing the *UAS-RferOR1* line to the $Or67d^{GAL4[2]}$ line (Kurtovic et al., 2007). Genomic integration and expression of *RferOR1* in *Drosophila* were verified using PCR and RT-PCR of *Drosophila* genomic DNA and antennal RNA, respectively.

2.6 | Single-sensillum recordings and odor simulation

Single-sensillum recordings (SSRs) on the at1 sensilla of 2- to 5-day-old flies were performed following standard procedures (De Fouchier et al., 2015). During SSRs, flies were kept alive under a constant 1.5 L/min flush of charcoal-filtered, humidified air delivered to the antenna. A wide range of weevil and palm beetle aggregation pheromone compounds (see details in Table S5) and structurally related chemicals, including the two components of the RPW pheromone ferrugineol (>98% purity, ChemTica Int.) and ferrugineone (>98% purity, ChemTica International), were tested to draw the response spectra of ORNs expressing *RferOR1* (Methods S1). The pheromone compound's purity was analysed in an Agilent Systems Model 6850 Gas Chromatography (GC) (injector temperature 250°C, detector temperature 250°C) using a flame ionization detector (FID) used for the analysis (HP-5 column: 30 m x 0.32 mm ID with 0.25 µm film thickness, with a temperature programme 60°C for 2 min, 25°C/min until 260°C, then 260°C for 5 min, and the carrier gas was helium with a linear velocity of 30 cm/s) (see GC-FID analysis in Figures S1a,b). Further, we conducted mass spectrometry (MS) analyses of the response-elicited-samples in the SSR studies to determine traces of contaminants, if any (see GC-MS analysis in Figure S1c).

All molecules were dissolved in *n*-hexane (100 ng/µl, 1 µg loaded on a filter paper inside the stimulus cartridge), and cartridges containing only hexane or 10 µg of 11-*cis*-vaccenyl acetate (cVA), the ligand of the *Drosophila* receptor OR67d, were used as controls. We performed dose-response analyses with increasing amounts of 0.1, 1, 10, 100 and 1000 ng of each molecule on filter paper strips for the most potent ligands identified. Stimulations lasted 500 ms, and the responses of at1 ORNs expressing *RferOR1* were calculated by subtracting the spontaneous firing rate (measured over 500 ms before stimulation) from the firing rate during the stimulation. Responses to the different stimuli were compared to the response to solvent alone using Kruskal-Wallis ANOVA followed by Dunn's post hoc test with Past v.3.26 (Hammer et al., 2001).

2.7 | *RferOR1* expression according to RPW age

RferOR1 expression was measured in male and female adult RPWs of different ages (0, 20, and 60 days old) using RT-qPCR, under the same conditions as described above. The relative expression levels of *RferOR1* were calculated with the $2^{-\Delta\Delta Ct}$ method by normalizing them to house-keeping genes (tubulin and β-actin) and the laboratory-reared males as reference.

2.8 | Structural modelling and docking of *RferOR1*

The *RferOR1* protein sequence was used to model the 3-dimensional (3D) structure of *RferOR1* using the homology modelling server I-TASSER (https://zhanglab.ccmb.med.umich.edu/I-TASSER/). After that, the Computed Atlas of Surface Topography of proteins (CASTp) webserver (http://cast.engr.uic.edu9) was used to identify potential binding pockets in the protein. The CASTp data were analysed as reported (Cali & Persaud, 2020). EADock DSS software from the SwissDock server provided by the Swiss Institute of Bioinformatics (http://swissdock.vital-it.ch/docking) was used to dock the target ligands into the *RferOR1* protein. The resulting docking predictions were viewed and analysed using the SwissDock server plugin in UCSF Chimera as reported in (Cali & Persaud, 2020). Twenty-nine target ligands, including the two RPW aggregation pheromone components and structurally related chemicals (including those tested on *RferOR1* expressed in *Drosophila* ORNs), were used for the docking experiments (as detailed in Table S8).

3 | RESULTS

3.1 | *RferOR* phylogeny and expression analyses

Thanks to sequencing of the RPW antennal transcriptome, we previously annotated 71 nonredundant candidate *R. ferrugineus* ORs (Antony et al., 2016) (Table S2). A maximum likelihood tree of Coleoptera ORs was constructed and revealed that the 71 *R. ferrugineus* ORs were clustered in four (1, 2, 5, and 7) of the seven major OR groups already described (Yuvaraj et al., 2021), with the largest number of *RferORs* found in group 7 (35 ORs), followed by groups 1 (14 ORs), 2A (14 ORs), 2B (4 ORs), 5A (3 ORs) and 5B (1 OR), which is not dissimilar to the OR distribution in the Curculionidae species *D. ponderosae* and *I. typographus* (Figure 1). *R. ferrugineus* lacked ORs in groups 3, 4, and 6. The phylogenetic analysis also indicated that several *R. ferrugineus* ORs display a 1:1 orthologous relationship with *D. ponderosae* and *I. typographus* ORs, with >95% bootstrap support (Figure 1). The functionally characterized pheromone receptors (PRs) from *I. typographus* (Yuvaraj et al., 2021) and *M. caryae* (Mitchell et al., 2012) were located in different clades (Figure 1). We identified *RferOR38* and *43* as possible orthologues of the two ItypPRs (within group 7), *RferOR56* as the orthologue of *McarOR20* (group 1), *RferOR24*, and *RferOR67* as the orthologues of *McarOR3*,

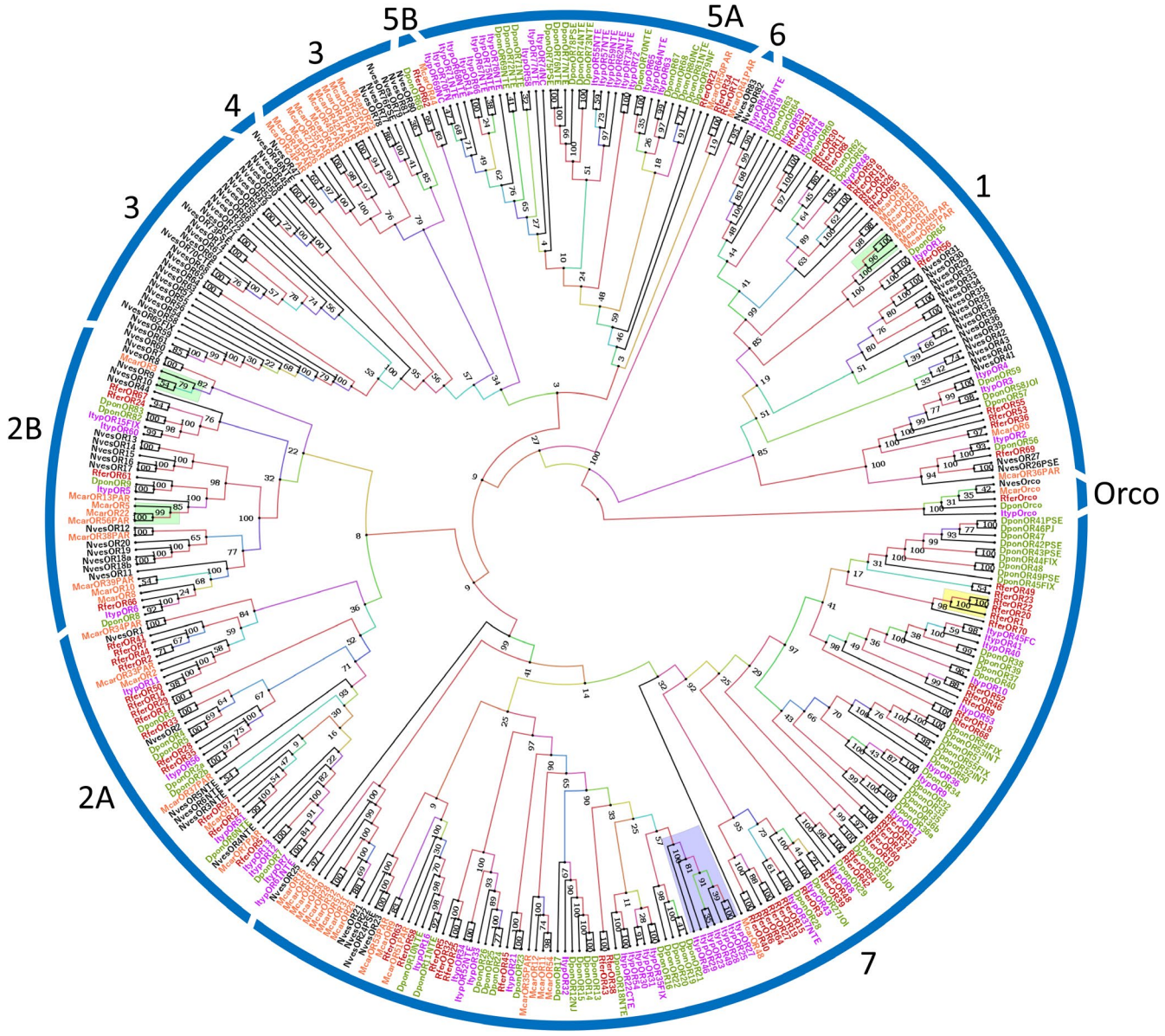

FIGURE 1 Maximum likelihood consensus tree of odorant receptors (ORs) from Coleoptera. The tree was built from the alignment of OR amino acid sequences of *Rhynchophorus ferrugineus*, Rfer (red) and the following coleopteran species: Nicrophorus vespilloides, Nves (black); *Ips typographus*, Ityp (magenta); *Dendroctonus ponderosae*, Dpon (green), and *Megacyllene caryae*, Mcar (orange). The Orco clade was used as an outgroup. The major coleopteran OR subfamilies are indicated with blue arcs and numbers. Clades containing functionally characterized ORs are highlighted in yellow (*RferOR1*, *R. ferrugineus*), blue (*I. typographus* ORs), and green (*M. caryae* ORs). Numbers on the branches are bootstrap values (RAxML; *n* = 100). The phylogenetic tree was visualized using FigTree (http://tree.bio.ed.ac.uk/software/figtree/), and branch appearance was coloured based on the bootstrap values. Scale = 3.0 amino acid substitutions per site. DponOR66 and probably RferOR62 in group 5B differ from that in previous studies (DponOR66 in group 5A in Andersson et al., 2019; Mitchell et al., 2020), perhaps because of the absence of ORs from additional species to correctly anchor groups 5A/5B

and *RferOR61* as the orthologue of *McarOR5* (group 2B). Phylogeny identified *RferOR62* as the orthologue of *DponOR66* from *D. ponderosae* (99% bootstrap support), and both were found clustered with *McarOR44* (group 5B, with 83% bootstrap support) from *M. caryae* (Mitchell et al., 2020).

Using RT-PCR, we next verified the expression of each of the *RferOR* genes in the antennae of females and males and in other tissues in males (Figure S2). We identified seven *RferOR* genes ubiquitously expressed in all tissues studied, five with no expression in the wings but expression in all other body parts, 20 with antennae-specific expression (*RferOR1* to *20*), one candidate male-biased OR (*RferOR32*), and the remaining *RferOR* genes with various expression patterns (Figure S2). Then, we quantified the expression levels of the 20 antennae-specific *RferORs* in male and female antennae of laboratory-reared animals (Table S2). They displayed various expression levels ranging from 0.001 to 5.24 of average ΔCt values

(normalized to tubulin and β-actin gene expression). A group of eight *RferORs* (*RferOR1* to *7* and *RferOR14*) exhibited visibly higher expression levels than the others (Table S2). Five of them belong to subfamily 7 (*RferOR1* and *RferOR3* to *6*), and three belong to subfamily 2A (*RferOR2*, *RferOR7*, and *RferOR14*) (Figure 1).

3.2 | *RferOR1* is overexpressed in response to pheromone pre-exposure

To identify *RferORs* potentially involved in detecting the aggregation pheromone, we next measured whether any *RferOR* gene expression levels were upregulated by pre-exposure to a synthetic pheromone blend for 4 h. Overall, changes in the expression patterns of the 20 antennae-specific ORs in the pheromone pre-exposed group compared to the control group were relatively minor (normalized to tubulin and β-actin gene expression) (Figure S3). Most ORs showed no change in expression or lower expression compared to that in nonexposed laboratory RPW controls (Figure 2a), whereas *RferOR1* was found to be marginally upregulated in pheromone pre-exposed RPWs (Figure 2a). Interestingly, the expression level of *RferOR1* upon pre-exposure ($2^{-\Delta\Delta Ct}$ values—normalized with endogenous control and using nonexposed RPW control as reference) was on par with that in the field-collected RPWs (Figure 2b), which are assumed to be under constant pheromone exposure in the field. *RferOR1* expression in the pheromone-exposed and field RPW groups was higher than the expression of all other 19 *RferOR* genes (*RferOR2* to *RferOR20*), based on Waller-Duncan analysis (Figure 2a).

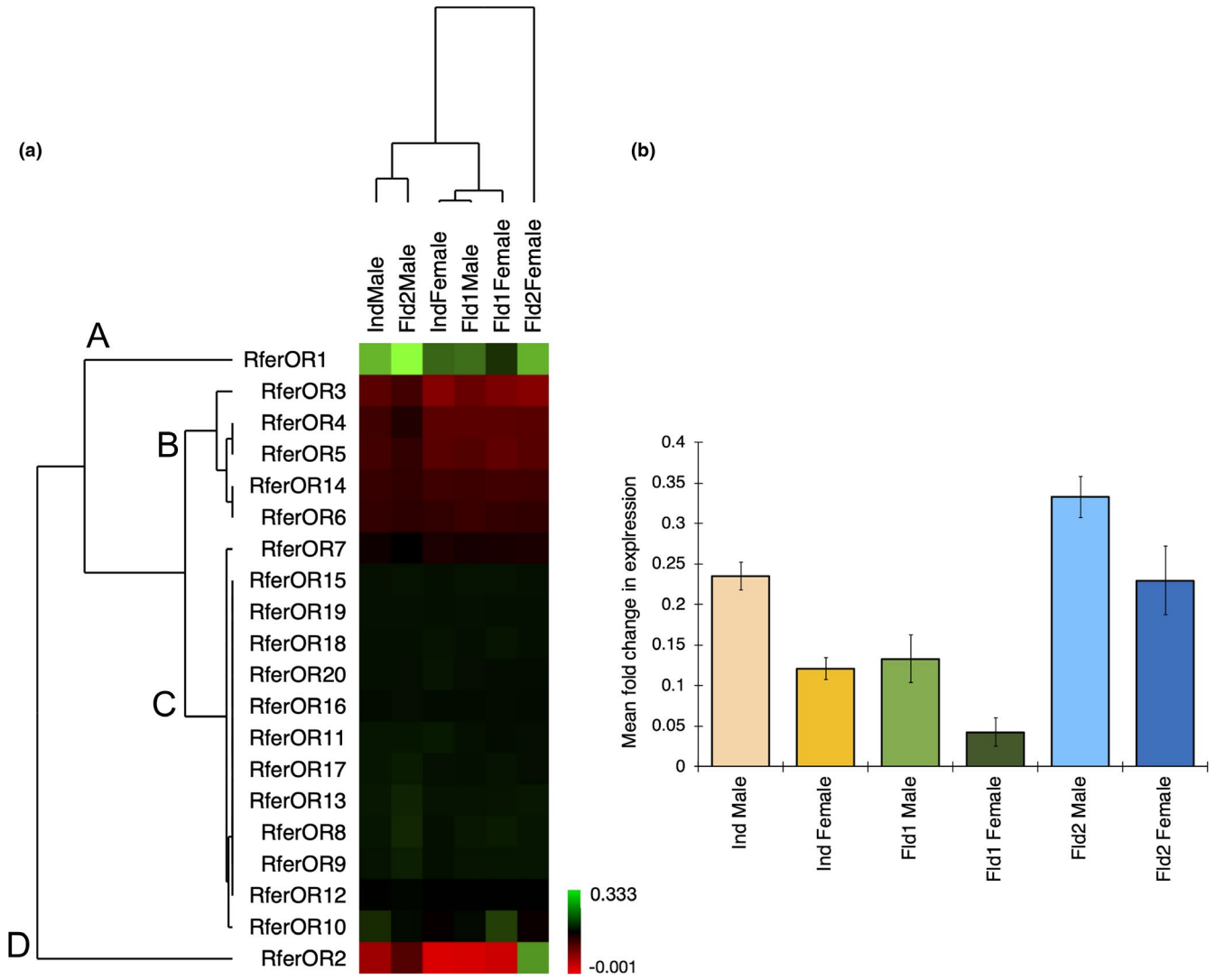

FIGURE 2 *RferOR1* is overexpressed in response to pheromone pre-exposure. (a) Heatmap showing changes in *RferOR* expression levels in pre-exposed and field-collected animals compared with the RferOR respective expression in nonexposed animals from the laboratory colony. Ind, insects pre-exposed with a commercial aggregation pheromone; Fld1 and Fld2, insects collected from two different date palm fields in Saudi Arabia. The data represents log-transformed $2^{-\Delta\Delta Ct}$ values measured by RT-qPCR. *RferOR* genes have been clustered following changes in expression. The heatmap colours represent expression level from highest (green) to lowest (red) expression. (b) Mean fold changes in *RferOR1* expression in pheromone pre-exposed and field-collected RPWs compared with insects from the laboratory colony. The relative expression of all other antennae-specific *RferORs* is provided in Figure S3

3.3 | *RferOR1*-silenced RPW adults exhibit a reduced response to pheromone

Based on the results of *RferOR* expression analyses, we focused on the six most highly expressed *RferORs* and further investigated their potential contribution to pheromone detection, with the aim of identifying pheromone receptor candidates. To do so, we used gene silencing with RNA interference. Injection of dsRNA successfully knocked down the expression of the six *RferOR* genes, with knockdown efficiencies of between 75% and 80% ($2^{-\Delta\Delta Ct}$ value) when compared to noninjected controls (Figure 3a).

The behaviour of *RferOR*-silenced RPWs in response to a commercial aggregation pheromone was measured in Y-maze olfactometers. In these behavioural assays, *RferOR1*-silenced animals showed significant behavioural changes in response to a commercial aggregation pheromone compared to the behaviour of controls. We found that 56.25% of *RferOR1*-silenced RPWs were unable to respond to pheromone stimuli, as the adults were not responding to the pheromone stimuli and moved towards clean air, 31.25% had no response at all (Figure 3b). Only 12.5% of the *RferOR1*-silenced animals were attracted to the pheromone, a significantly smaller proportion than that of the noninjected controls (79.17%) and NFW-injected controls (75%) ($p < .001$; Table S3). *RferOR1*-silenced insects also had

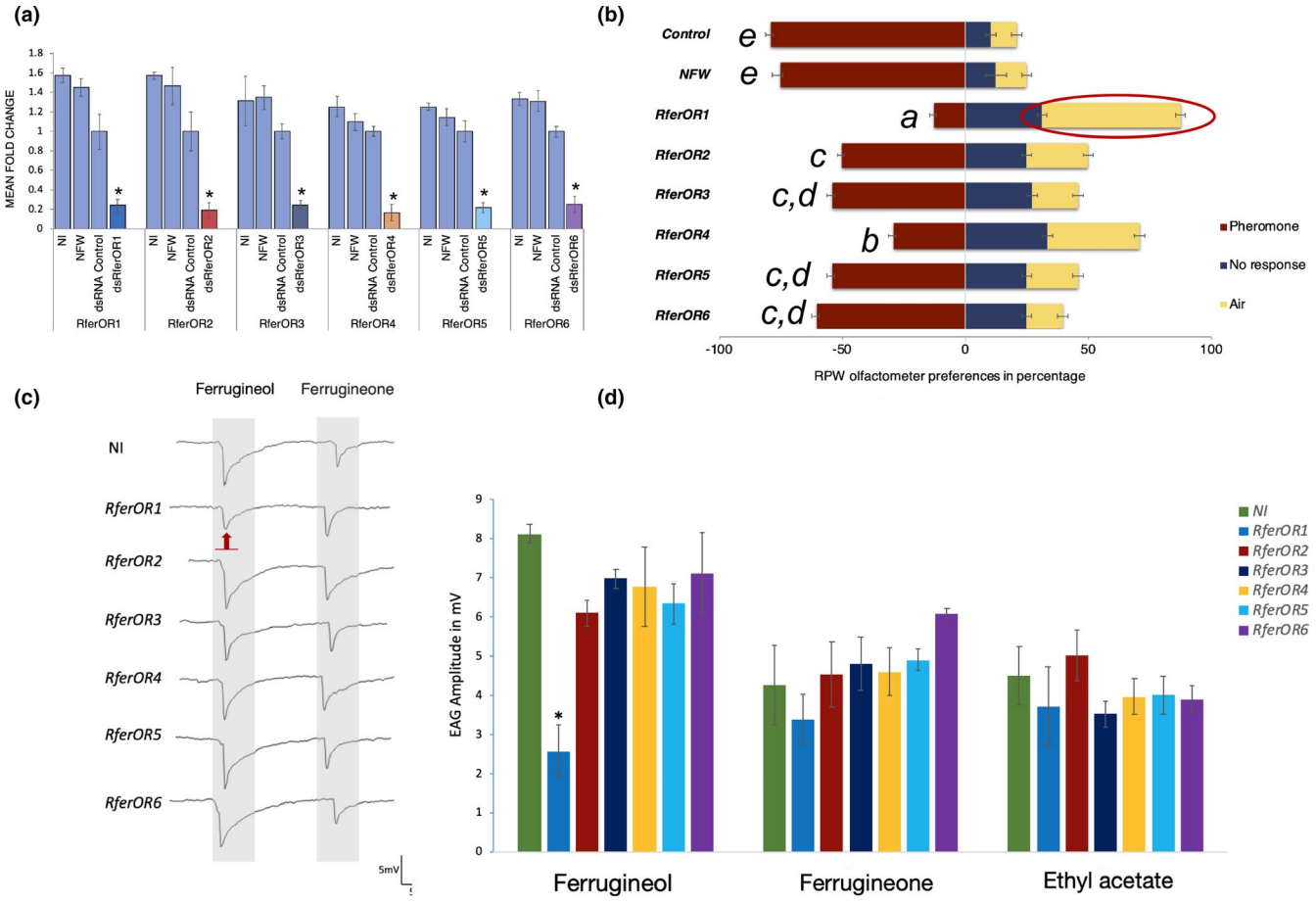

FIGURE 3 Pheromone response is altered in *RferOR1*-silenced RPWs. (a) Effects of RNAi based silencing on *RferOR* expression, measured using qRT-PCR. Data presented as mean fold change in each RferOR expression ($2^{-\Delta\Delta Ct}$ values) using dsRNA control as reference (abbreviations: NI, noninjected; NFW, nuclease free water injected; dsRNA Control, negative control dsRNA injected and dsRferOR; respective *RferOR* dsRNA-injected). (*) represents the statistical significance measured *at* $p < 0.05$ and error bars represents SEM ($p < .05$; one-way ANOVA with LSD). (b) Effects of RNAi on behaviour. Olfactometer preferences exhibited by OR-silenced (*RferOR* dsRNA-injected) RPWs against NI (Control) and NFW-injected insects to pheromone (Supporting Information Methods). Responses were provided as "towards pheromone" (red), "no response" (blue), and "towards air" (yellow) expressed as a percentage of the total ($n = 16$). *RferOR1*-silenced adults showing significant response "towards air" is highlighted with an oval circle (see Table S3). Error bars represent SEM, and letters (a, b, c, d, and e) represent five homogenous subsets identified by Waller-Duncan statistical analysis. (c). Representative EAG recordings from the *RferOR*-silenced insects compared with noninjected (NI) weevils. Grey columns represent the stimulus duration. The red arrow indicates a reduction in EAG response in *RferOR1*-silenced insects when stimulated by ferrugineol. (d). EAG amplitudes measured from RNAi *RferOR*-silenced and noninjected (NI) insects when stimulated with 200 ng on the filter paper of the aggregation pheromone components ferrugineol and ferrugineone and with volatile ethyl acetate ($n = 16$) (mean values ±SEM).* $p < .001$ (one-way ANOVA followed by a Tukey's HSD method) indicates a significant reduction in *RferOR1*-silenced insect response to ferrugineol compared to NI (see Table S4). Error bars represent SEM

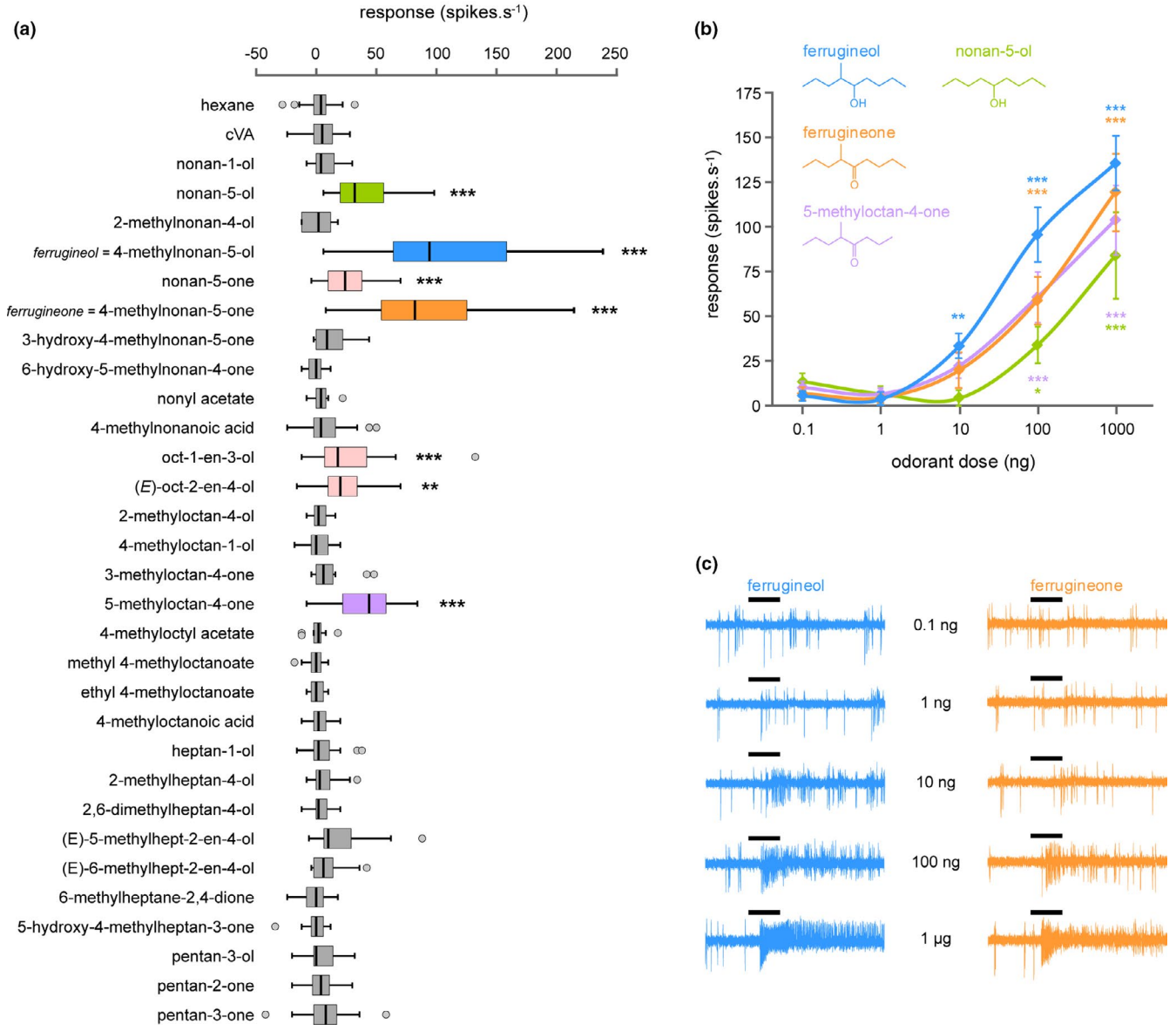

FIGURE 4 *RferOR1* is activated by ferrugineol, ferrugineone, and five other structurally related compounds. (a) Action potential frequency of Drosophila at1 ORNs expressing *RferOR1* when stimulated with a panel of pheromone compounds and related chemicals (1 µg loaded in the stimulus cartridge). Box plots show the median and the first and third quartiles of the distribution (n = 14–38). $^{**}p < .01$, $^{***}p < .001$, significantly different from the response to solvent alone (Kruskal-Wallis ANOVA followed by a Dunn's post hoc test). (b) Dose-response curves of Drosophila at1 ORNs expressing *RferOR1* to the four most active compounds. Data represented are mean action potential frequencies ±SEM (n = 9–15). $^{*}p < .05$, $^{**}p < .01$, $^{***}p < .001$, significantly different from the response to solvent alone (Kruskal-Wallis ANOVA followed by a Dunn's post hoc test). (c) Single sensillum recordings obtained for a Drosophila at1 ORNs stimulated with increasing doses of ferrugineol and ferrugineone. Black bars represent the duration of the stimulus (500 ms)

significantly different responses than other *RferOR*-silenced insects (p = .001). Waller-Duncan analysis for homogenous subsets confirmed *RferOR1* and *RferOR4* as separate subsets *a* and *b*; *RferOR2*, *RferOR3*, *RferOR5*, and *RferOR6* as subsets *c* and *d*; and the controls NI and NFW as subset *e* in response to commercial aggregation pheromone (Figure 3b). Similarly, with their reduced response to pheromone, *RferOR1*-silenced insects were grouped as a homogenous subset. The olfactometer study results revealed that the most altered pheromone behavioural response was obtained when *RferOR1* was silenced.

For each of the six *RferOR*-silenced RPW groups, we also recorded electroantennograms (EAG) of 21-day-old animals following stimulation with the pheromone components ferrugineol, ferrugineone, and with ethyl acetate, a host volatile known to be highly active on RPW antennae (Guarino et al., 2011). As shown in Figure 3c,d, and Table S4, responses to ethyl acetate were not statistically different between the experimental groups (noninjected and *RferOR*-silenced

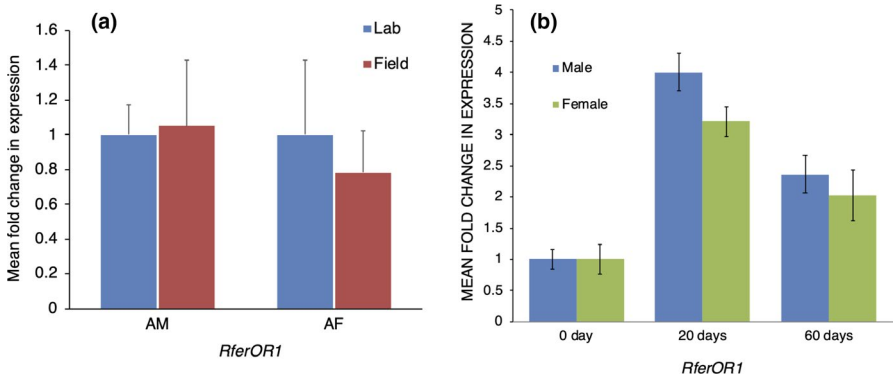

FIGURE 5 *RferOR1* expression according to age. (a) Relative expression of *RferOR1* in antennae from RPW male and female adults (RT-qPCR) (fold changes compared to the expression level in laboratory-reared male antennae). (b) *RferOR1* relative expression in antennae of 0, 20, and 60-day-old RPW male and female adults (fold changes compared to the expression level in antennae of 0-day old laboratory-reared males)

animals), suggesting that the dsRNA treatments did not alter the overall antennal sensitivity. Similarly, responses to the pheromone compound ferrugineone did not differ between the different groups (Figure 3c). However, *RferOR1*-silenced insects exhibited a significantly reduced response to ferrugineol, with a mean EAG amplitude of 2.57 (±0.67) mV compared to that of 8.12 (±0.42) mV in control insects ($p < .001$; Table S4) (Figure 3c). All other *RferOR*-silenced experimental groups showed unaltered EAG responses to ferrugineol (Figure 3c). Overall, these results suggested that *RferOR1* may likely be involved in ferrugineol detection.

3.4 | 3.4 Transgenic *Drosophila* olfactory neurons expressing *RferOR1* respond to ferrugineol and ferrugineone

Based on its high expression level and marginal overexpression upon pheromone pre-exposure and the reduced antennal and behavioural responses to pheromone following its knockdown by RNA interference, *RferOR1* appeared to be the best candidate *R. ferrugineus* pheromone receptor. For further confirmation, we heterologously expressed a *RferOR1* transgene in *D. melanogaster* ORNs from the at1 sensilla deprived of the endogenous OR67d, which is tuned to cVA (Kurtovic et al., 2007), and performed single-sensillum recordings. We first verified the lack of response to cVA in transformed *Drosophila* at1 ORNs, confirming the absence of OR67d (Figure 4a). Then, the ORNs were stimulated with high doses of ferrugineol, ferrugineone (>98% purity of both pheromone compounds verified through GC-FID analysis, Figure S1), and a range of pheromone compounds from other species of weevils or palm beetles (Table S5) and structurally related compounds. We found strong responses to ferrugineol and ferrugineone (mean responses of 106 and 95 spikes/s, respectively) and minor responses to nonan-5-ol, nonan-5-one, oct-1-en-3-ol, (*E*)-oct-2-en-4-ol and 5-methyloctan-4-one (Figure 4a). We excluded that these minor responses were due to contamination of the synthetic compounds by traces of pheromone by GC-MS analysis (Figure S1c). We next carried out dose-response experiments for the four most active compounds. Ferrugineol appeared to be the best *RferOR1* agonist as it significantly activated *RferOR1*-expressing ORNs starting at a dose of 10 ng (Figure 4b,c). Ferrugineone, 5-methyloctan-4-one and nonan-5-ol induced significant responses at doses of 100 ng and 1 µg. With those experiments, we thus confirmed that *RferOR1* is involved in pheromone detection in *R. ferrugineus*.

3.5 | *R. ferrugineus* pheromone receptor expression was observed throughout the life cycle

We observed a slight difference in *RferOR1* expression patterns between male and female antennae; however, the values were not significantly different and thus did not show sex-biased expression, in accordance with our tissue-specific expression analysis (Figure 5a). Importantly, *RferOR1* expression was observed throughout the life cycle (0–60 days), with maximal expression at 20 days. At 60 days, *RferOR1* expression was higher than that in newly emerged RPWs (0 days) (Figure 5b).

3.6 | Structural modelling and molecular docking of *RferOR1*

The 1233 bp open reading frame (ORF) of *RferOR1* encodes a protein of 411 amino acid residues whose structure was modelled (Figure 6a). We identified a total of 94 pockets, with the main binding pocket (the probable active site) predicted to be made up of 28 amino acid residues (Table S6), of which 14 (Table S7) are hydrophobic (50%), seven are hydrophilic (25%), two are positively charged (7.14%), and five are negatively charged (17.86%) (Figure S4). In *RferOR1*, the channel to the active site had a distinct entry mouth and exit mouth. The pocket had two mouth openings (Table S6); the residues making up the entry mouth (Table S7) were D77, K78, D298, K301, V302, and D308, while those making up the exit mouth

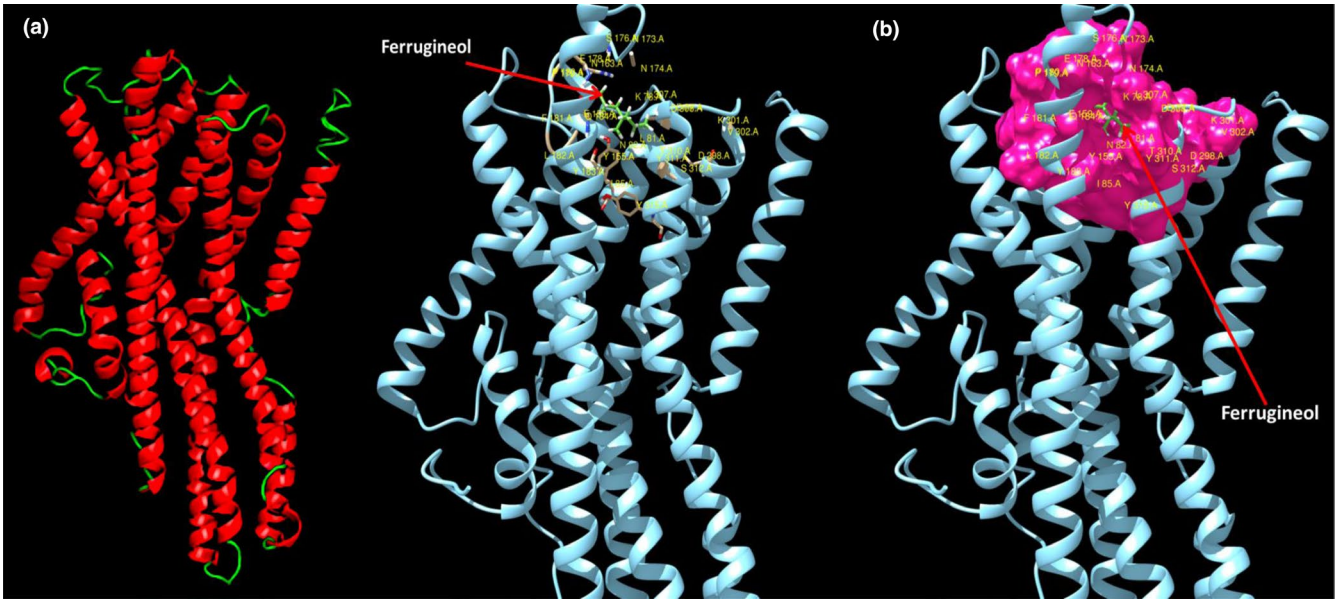

FIGURE 6 Structural modelling and docking of red palm weevil pheromone receptor, *RferOR1*. (a) Cartoon presentation—Helix and Loop of the structure. The figures were rendered using molecular visualization software PyMOL (Schrödinger). (b) Binding of aggregation pheromone 4-methyl-5-nonanol (ferrugineollabelled in green) to the binding pocket of *RferOR1* (left and right). In the right panel, the pocket is shown in hydrophobicity surface representation and coloured in dark pink

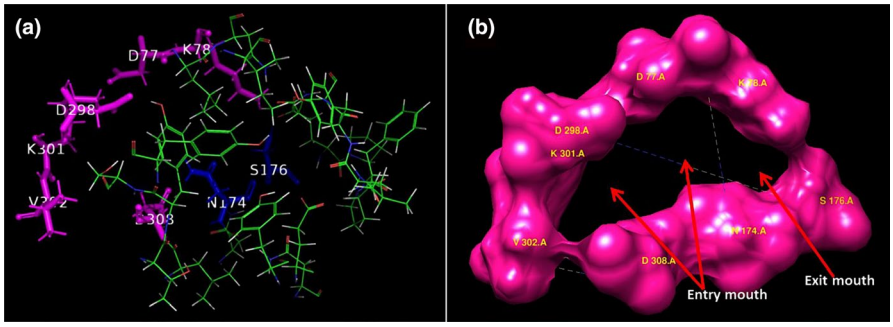

FIGURE 7 Mouth openings for the active site of *RferOR1*. (a) Residues making up the entry mouth are shown in magenta, while residues making up the exit mouth are shown in blue, while in (b), the mouths are shown interactively (hydrophobicity surface). In *RferOR1* the active site channel has a distinct entry mouth and an exit mouth. The residues making up the entry mouth are D77, K78, D298, K301, V302, and D308, while those making up the exit mouth are N174 and S176

were N174 and S176 (Table S6 and Figure 7a,b). These features of the active site are summarized in Table S7.

We then conducted docking studies using the different compounds used to challenge *RferOR1* expressed in *Drosophila* (Table S8), five additional related compounds, and VUAA1, an Orco agonist (Jones et al., 2011). The most energetic binding pocket-binding mode was selected for each ligand, and the binding energy (Table S9) was used to define the protein binding affinity towards a given molecule.

With the exception of VUAA1 (which was included as a negative control), all other molecules bound within the active site of the protein, giving negative binding energies (Figure 6b). The lower the binding energy was, the stronger the binding was (higher affinity) and vice versa. As an example, Figure 6b illustrates the binding of a ferrugineol molecule to the active site of the receptor. All tested ligands except VUAA1 were able to fully penetrate the binding pocket (Figure S5). Comparing the two aggregation pheromone components, the receptor showed a slightly higher affinity towards ferrugineol (binding energy, −31.73 kcal/mol) than ferrugineone (−28.89 kcal/mol) did (Table S8). Within the active site, seven (out of the 28) residues made direct interaction with ferrugineol (15 total interactions) or ferrugineone (13 total interactions); the common residues for both ligands were L81, Y155, N174, P180, and Y311 (Table S10 and Figure S6). Residues E178, Q184 interact with the only ferrugineol, while Q159 and N163 interact with the only ferrugineone. N174 was one of two residues (the other being S176) that makes up the active site exit mouth (Table S6 and Figure S6). The above receptor-ligand interaction differences may explain why the receptor showed a slightly higher affinity towards ferrugineol compared to ferrugineone.

4 | DISCUSSION

In recent years in the Anthropocene epoch, many unpredicted and irreversible changes in insect pest distribution and behaviour have occurred, and some insect species have, with human help, spread rapidly across the world. The phenomenal expansion and global spread of the RPW in almost all dominant palm tree-growing countries over the last three decades has recently resulted in its attainment of category-1 pest status (EPPO, 2019) as a consequence of the commercial exchange of palm trees worldwide (Al-Dosary et al., 2016; Faleiro, 2006; Peri et al., 2017). In the palm weevil, both long-range attraction and host colonization for feeding and mating are regulated by an aggregation pheromone (Peri et al., 2017; Vacas et al., 2017). Understanding the molecular mechanism of pheromone reception and elucidating the functional role of pheromone-specific ORs and odorant-binding proteins (OBPs) may help to design novel pest management solutions (Picimbon, 2019; Venthur & Zhou, 2018). In this study, from 71 candidate RPW ORs, we identified one OR, *RferOR1*, as a pheromone receptor in *R. ferrugineus*. We demonstrated pheromone response disruption through RNAi-based gene silencing and confirmed the functional role of *RferOR1* in pheromone detection through heterologous expression in *Drosophila*. These findings provide the first insights into the molecular basis of chemoreception in a palm weevil species. They also represent a significant advance towards a better understanding of the molecular bases of olfaction in Coleoptera. While insects from this order, including phytophagous beetles of economic importance, pathogen vectors, predators and beneficial insects with key roles in the cycle of organic matter, exhibit a wide range of ecologies, it is surprising that only five other ORs in this order have been functionally characterized to date (Mitchell et al., 2020; Yuvaraj et al., 2021).

Because of the paucity of functional data on Coleoptera ORs (Mitchell et al., 2020), we had to rely on several approaches to select ORs possibly involved in pheromone detection. First, we employed a phylogenetic approach to identify a coleopteran-specific pheromone receptor (PR) clade. However, the five Coleoptera ORs described as PRs did not cluster in the same clade in the phylogenetic tree (Figure 1), precluding the identification of good RPW PR candidates. In fact, it has been proposed that coleopteran PRs are highly divergent and have acquired unique functions related to different pheromone compounds, contrary to lepidopteran PRs, which cluster in specific clades in accordance with structural similarity among pheromone compounds (Andersson et al., 2015; Mitchell et al., 2020). As PRs in insects are usually characterized by high transcript abundance and specific expression in the antenna, we followed these criteria to select candidate ORs via tissue expression studies and quantification of relative OR expression. After that, we targeted the ORs that were highly and uniquely expressed in the antennae for further studies. We also used another criterion, which is transcript upregulation upon exposure to pheromone stimuli. With all these criteria, we selected six highly expressed ORs for gene silencing. We found a correlation between the reduction in *RferOR1* transcript level and a reduction of the antennal response to the pheromone, suggesting that *RferOR1* was the best candidate pheromone receptor. However, electrophysiology and behavioural assays represent the antennal and the animal level, respectively, and cannot account for OR function (molecular level). Thus, we ultimately confirmed by heterologous expression in *Drosophila* ORNs that *RferOR1* is a receptor sensitive to ferrugineol and ferrugineone. In doing so, here, we provide the first evidence that *Drosophila* ORNs can be used efficiently for the study of ORs from Coleoptera, in addition to Diptera and Lepidoptera. Indeed, the function of previously characterized Coleoptera pheromone receptors was determined via their expression in *Xenopus* oocytes or HEK cells, which are in vitro methods that proved successful for ligand identification of ORs from species from a range of insect orders.

The specificity of *RferOR1* towards the RPW pheromone was further assessed by challenging *Drosophila* ORNs with a wide range of compounds of various chain lengths (5°C to 9°C) and functional groups (Figure 4). Fly ORNs presented a high sensitivity to the two components of the RPW aggregation pheromone (Figure 4b) and sensitivity to a lesser extent to five structurally related compounds (nonan-5-ol, nonan-5-one, oct-1-en-3-ol, (*E*)-oct-2-en-4-ol, and 5-methyloctan-4-one). We excluded that these minor responses are due to contaminations with RPW pheromone components, as confirmed by GC-MS analysis (Figure S1c). One of these compounds, nonan-5-ol, is a component of the pheromone of *Metamasius hemipterus*, another Rhynchophorinae (Perez et al., 1997). RPW and *M. hemipterus* are not sympatric species, however, suggesting that nonan-5-ol does not interfere with RPW pheromone communication in the wild. Similarly, (*E*)-oct-2-en-4-ol is a pheromone component of the related species *R. palmarum*, whose native range extends from Central to South America. Of importance, none of the tested pheromones from weevil species living in sympatry with the RPW was detected by *RferOR1*, suggesting the maintenance of species isolation.

Alternatively, it is possible that *RferOR1* tuning is altered by the perireceptor space composition of *Drosophila* t1 sensilla and that the minor responses observed result from an inadequate environment. Indeed, pheromone receptors in insects have been shown to be usually quite specific (Breer et al., 2019; Fleischer & Krieger, 2018, 2020; Leal, 2013), but our study revealed that *RferOR1* was not strictly tuned to pheromone compounds. Such phenomenon has already been observed for Lepidoptera pheromone receptors when heterologously expressed in t1 (De Fouchier et al., 2015), but response profile comparison between heterologous ORs and native ORNs revealed that, although ORNs are more specific, the main ligand(s) remain the same. For instance, it is known that OBPs enhance the specificity and sensitivity of ORs (Große-Wilde et al., 2006, 2007), and the OBPs present in *Drosophila* t1 are probably not the same as in RPW pheromone sensitive sensilla. Similarly, the absence of adequate pheromone-degrading enzymes in *Drosophila* t1 may explain the observed continuous spiking after stimulation with high pheromone doses (1 µg). Without pheromone degradation in t1, the ORNs would be continuously stimulated. Similar effects of prolonged stimulation were observed in earlier studies using expression in *Drosophila* (De Fouchier et al.,

2017; Syed et al., 2006). Comparison with the response profile of RPW pheromone sensilla via SSR will ultimately answer these questions. The hypotheses described above may also explain the apparent discrepancy between the RNAi results and *RferOR1* tuning. *RferOR1 Drosophila* responded to ferrugineol and ferrugineone, whereas *RferOR1* knockdown through RNAi in vivo animal impaired electrophysiological responses to ferrugineol only. Either *RferOR1* response to ferrugineone when heterologously expressed in *Drosophila* results from less specificity due to a not optimal OR environment, or it exists another *RferOR* (or ORs) tuned to ferrugineone in RPW antennae that remain to be identified.

Interestingly, *RferOR1* was found to be expressed throughout the RPW lifespan, with its highest expression observed in adults at 20 days of life, correlating with the highest *RferOrco* expression (Soffan et al., 2016), which was recorded at the same age. This phenotype correlates well with the previous observation that adult mating success is independent of age (Abdel-Azim et al., 2012). As pheromone reception and response are directly linked to reproductive success, this feature might have helped the phenomenal expansion of palm weevils worldwide.

Our docking studies based on binding energies defined the affinity of *RferOR1* towards the RPW pheromone (Table S9). We decoded pheromone-*RferOR1* interactions using in silico docking, and the results predicted that *RferOR1* responds to ferrugineol and ferrugineone with high binding affinity, as observed experimentally in the *Drosophila* system. The difference in binding energies between the two aggregation pheromone compounds was not significant, but the binding energy towards ferrugineol was slightly higher than that towards ferrugineone (Table S9). This agrees with the observation that the active site features of *RferOR1* that respond to both pheromone compounds are slightly different (Table S10). This suggests that the active site features of *RferOR1* that respond to both pheromone compounds are quite similar. It will be interesting and useful in the future to characterize the binding pockets to test the above hypothesis. Moreover, the critical amino acid residues involved in the formation of ferrugineol–*RferOR1* complexes need to be validated by subsequent site-directed mutagenesis and fluorescence binding assays. Differences in affinities of the receptor to different ligands could also be attributed to the size and nature of the compounds tested with respect to the size and nature of the active site of *RferOR1* (Table S9, Figure 7 and S4). For example, a molecule such as ferrugineol (MW =158.28) can fully access the active site of the receptor (Figure S5) with a binding energy of −31.73 kcal/mol (Table S9). However, the molecule VUAA1 (MW =367.47), which is 2.3-fold larger in size than ferrugineol, cannot access the pocket (Figure S5), giving a positive binding energy of 30.16 kcal/mol (Table S9).

The primary purpose of our *RferOR1* docking experiment was to obtain acceptable models of OR-ligand complexes (especially *RferOR1*-ferrugineol), for which no experimental structures are available, and to predict potential binding pockets and the active site of *RferOR1*. Because several studies indicated that subtle changes in the binding site compositions of ORs result in differential odorant binding and odor detection (Harini & Sowdhamini, 2015; Yan et al., 2020), the paucity of information on deorphanized insect ORs in the database may lead to the poor prediction of protein affinity towards a given ligand (Harini & Sowdhamini, 2015). Hence, docking screening results based on binding energies still wait for more functional studies to be validated (Chen, 2015). Indeed, comparison to come with additional OR function, structure, and binding site identification, especially within Coleoptera, will be useful for increasing the accuracy of predictions with regards to specificity and selectivity across a wider repertoire of ORs. The data presented here characterizing the *RferOR1* active site could be used in the future to investigate the roles of its constituent amino acid residues in ligand binding. Still, most importantly, these data could be used to design mutant variants that are more potent than the wild-type receptor for use as biosensors for early detection of the palm weevil in date palm fields. Preliminary energy analysis around the receptor's active site indicated that mutation of 12 residues (out of the 28 binding pocket) would potentially give 27 stable mutants (Table S11). All seven *RferOR1* active site channel mouth residues are part of these 12 residues (Tables S6 and S7; Figure 7), although only three (Y155, Q159, and N174) are in direct contact with the ligand within the active site (Table S10 and Figure S6). Only one out of the 12 residues are hydrophobic even though 50% of the active site residues are hydrophobic (Tables S6 and S7, and Figure S4). Out of the 27 potential stable mutants (Table S11), 25 (92.6%) were when the new residues were hydrophobic, two (7.4%) mutants when the new residues were negative, and none mutants were when the new residues were either positive or hydrophilic (Table S7). In the future, docking screening of the stable *RferOR1* mutant variants (Table S11) should be carried out to identify potentially better mutant variants than the wild type that could be ultimately developed as biosensors for early detection of the palm weevil infestation.

Looking back at the OR phylogenetic tree, we observed that *RferOR1* belongs to a monophyletic clade that groups two other antennae-enriched RPW ORs, *RferOR20* and *RferOR22*, and a ubiquitously expressed RPW OR, *RferOR70* (Figure 1). Whether these ORs also detect pheromone compounds remains to be determined, and this knowledge would provide a better understanding of pheromone receptor evolution in Curculionidae. Interestingly, we noticed that the C-terminal parts (amino acids 210–404) of *RferOR20*, *RferOR22*, and *RferOR1* are highly conserved, suggesting that these ORs have recently evolved from tandem duplications. This C-terminal part is predicted to be involved in ligand-binding sites in *RferOR1*, with noticeably 82% of the binding pocket residues being near the C-terminal end (Table S6). This suggests that *RferOR20* and *RferOR22* may also have pheromone receptor functions. Strikingly, the PRs characterized in the cerambycid beetle, *M. caryae*, (Mitchell et al., 2012) and the European spruce bark beetle, *I. typographus* (Yuvaraj et al., 2021), belong to distantly related OR clades (Figure 1). This highlights the diversity of pheromone receptors in beetles and suggests that pheromone receptors appeared several times during the evolution of Coleoptera.

5 | CONCLUSIONS

With the identification of a pheromone receptor tuned to the two components of the RPW aggregation pheromone, our findings represent a significant step forward in understanding the chemosensory mechanisms of the primary enemy of palm trees. Our study also defines the RPW as an essential model for exploring the chemical ecology of palm tree weevils and the evolution of pheromone detection in Coleoptera. By demonstrating that *Drosophila* ORNs can be reliably used for the functional expression of Coleoptera ORs and providing a standardized protocol for OR silencing via RNAi, we have opened a new workflow that can be applied to the deorphanization of other insects ORs. Finally, our study provides a characterized OR as a new target for RPW pest control. Our study provides experimental evidence that, on the one hand, silencing *RferOR1* may disrupt palm weevil aggregation in palm tree plantations, ultimately disturbing the reproductive process and decreasing the *R. ferrugineus* population, a promising step for preventing coordinated mass attacks. On the other hand, this OR could also be used for the development of biosensors, an E-nose, and behaviour-based robots by exploiting pheromone-*RferOR1* interactions for pheromone-based RPW monitoring in the field, allowing the early detection of infestations in date palm fields. The discovery of this OR also opens up the possibility of a "reverse chemical ecology" approach (Leal, 2013, 2017; Leal et al., 2008) based on the screening of new semiochemicals able to interfere with the OR response to the pheromone and ultimately with the behaviours of the RPW in the field.

ACKNOWLEDGEMENTS

Funding for this research—grant numbers: KACST-NSTIP 12-AGR2854-02 (MAARIFAH-KACST), KAUST-OSR-2018-RPW-3816–1, and OSR-2018-RPW-3816–4 of Saudi Arabia, and the ANR Investissements d'avenir program "PheroSensor" of France. The authors are grateful to the Deanship of Scientific Research, King Saud University, for funding through the Vice Deanship of Scientific Research Chairs. The authors thank Anne-Francoise J. Lamblin and T. A. Abrajano of KAUST-OSR for their invaluable support. The authors thank the date palm farmers in the Al Kharj and Al Qassim areas for their support in obtaining RPWs and advice in adult weevil collection. Jibin Johny is grateful for the researcher stipend and training provided by CDPR through 12-AGR2854-02 and OSR-2018-RPW-3816–1 projects. We also thank Jérémy Gévar (iEES, France) for GC-FID/MS analyses of standard compounds.

AUTHORS' CONTRIBUTIONS

Binu Antony, Emmanuelle Jacquin-Joly, Krishna Persaud, and Arnab Pain conceived of the study and acquired the grant. Jibin Johny, Binu Antony, and Mohammed Ali Al-Saleh participated in RPW field collection, rearing and electrophysiology. Binu Antony, Arnab Pain and Jibin Johny performed transcriptome, assembly and annotation. Binu Antony and Jibin Johny performed the silencing experiment. Nicolas Montagné, Rémi Capoduro, Binu Antony, and Emmanuelle Jacquin-Joly carried out the *Drosophila* functional expression studies. Khasim Cali, Krishna Persaud, and Binu Antony performed the docking experiment. Binu Antony wrote the paper with contributions from Nicolas Montagné, Jibin Johny, Emmanuelle Jacquin-Joly, Khasim Cali, and Krishna Persaud.

DATA AVAILABILITY STATEMENT

The *RferOR1* sequence reported in this paper has been deposited in the GenBank database (accession no. MK060009). *RferOR2-RferOR20* and *RferOR22* sequences are available in the Dataset S1.

ORCID

Binu Antony https://orcid.org/0000-0002-6292-620X
Jibin Johny https://orcid.org/0000-0002-2265-5046
Nicolas Montagné https://orcid.org/0000-0001-8810-3853
Emmanuelle Jacquin-Joly https://orcid.org/0000-0002-6904-2036
Khasim Cali https://orcid.org/0000-0002-2017-6922
Krishna Persaud https://orcid.org/0000-0001-5730-9568
Arnab Pain https://orcid.org/0000-0002-1755-2819

REFERENCES

Abdel-Azim, M. M., Vithal, P. S. P., Aldosari, S. A., & Mumtaz, R. (2012). Impact of mating frequency on fecundity, fertility and longevity of red palm weevil, *Rhynchophorus ferrugineus* (Olivier)(Coleoptera: Curuclionidae). *Journal of Agricultural Science and Technology*, *A*, *2*(4A), 520.

Al-Dosary, N. M. N., Al-Dobai, S., & Faleiro, J. R. (2016). Review on the management of red palm weevil *Rhynchophorus ferrugineus* olivier in date palm *Phoenix dactylifera* L. *Emirates Journal of Food and Agriculture*, *28*(1), 34.

Andersson, M. N., Keeling, C. I., & Mitchell, R. F. (2019). Genomic content of chemosensory genes correlates with host range in wood-boring beetles (*Dendroctonus ponderosae*, *Agrilus planipennis*, and *Anoplophora glabripennis*). *BMC Genomics*, *20*(1), 1–17.

Andersson, M. N., Löfstedt, C., & Newcomb, R. D. (2015). Insect olfaction and the evolution of receptor tuning. *Frontiers in Ecology and Evolution*, *3*, 53.

Antony, B., Johny, J., Abdelazim, M. M., Jakše, J., Al-Saleh, M. A., & Pain, A. (2019). Global transcriptome profiling and functional analysis reveal that tissue-specific constitutive overexpression of cytochrome P450s confers tolerance to imidacloprid in palm weevils in date palm fields. *BMC Genomics*, *20*(1), 440. https://doi.org/10.1186/s12864-019-5837-4

Antony, B., Johny, J., & Aldosari, S. A. (2018). Silencing the odorant binding protein RferOBP1768 reduces the strong preference of palm weevil for the major aggregation pheromone compound ferrugineol. *Frontiers in Physiology*, *9*, 252. https://doi.org/10.3389/fphys.2018.00252

Antony, B., Soffan, A., Jakše, J., Abdelazim, M. M., Aldosari, S. A., Aldawood, A. S., & Pain, A. (2016). Identification of the genes involved in odorant reception and detection in the palm weevil *Rhynchophorus ferrugineus*, an important quarantine pest, by antennal transcriptome analysis. *BMC Genomics*, *17*, *69*. https://doi.org/10.1186/s12864-016-2362-6.

Benton, R., Sachse, S., Michnick, S. W., & Vosshall, L. B. (2006). Atypical membrane topology and heteromeric function of Drosophila odorant receptors in vivo. *PLOS Biology*, *4*(2), e20.

Bischof, J., Maeda, R. K., Hediger, M., Karch, F., & Basler, K. (2007). An optimized transgenesis system for Drosophila using germ-line-specific

φC31 integrases. *Proceedings of the National Academy of Sciences*, *104*(9), 3312–3317.

Breer, H., Fleischer, J., Pregitzer, P., & Krieger, J. (2019). Molecular mechanism of insect olfaction: Olfactory receptors. In J.-F. Picimbon (Ed.), *Olfactory concepts of insect control-alternative to insecticides* (pp. 93–114). Springer. https://doi.org/10.1007/978-3-030-05165-5_4

Butterwick, J. A., del Mármol, J., Kim, K. H., Kahlson, M. A., Rogow, J. A., Walz, T., & Ruta, V. (2018). Cryo-EM structure of the insect olfactory receptor Orco. *Nature*, *560*(7719), 447–452.

Cali, K., & Persaud, K. C. (2020). Modification of an Anopheles gambiae odorant binding protein to create an array of chemical sensors for detection of drugs. *Scientific Reports*, *10*(1), 1–13.

Chen, Y.-C. (2015). Beware of docking!. *Trends in Pharmacological Sciences*, *36*(2), 78–95.

Darriba, D., Taboada, G. L., Doallo, R., & Posada, D. (2011). ProtTest 3: Fast selection of best-fit models of protein evolution. *Bioinformatics*, *27*(8), 1164–1165.

De Fouchier, A., Sun, X., Monsempes, C., Mirabeau, O., Jacquin-Joly, E., & Montagné, N. (2015). Evolution of two receptors detecting the same pheromone compound in crop pest moths of the genus Spodoptera. *Frontiers in Ecology and Evolution*, *3*, 95.

de Fouchier, A., Walker, W. B., Montagné, N., Steiner, C., Binyameen, M., Schlyter, F., Chertemps, T., Maria, A., François, M.-C., Monsempes, C., Anderson, P., Hansson, B. S., Larsson, M. C., & Jacquin-Joly, E. (2017). Functional evolution of Lepidoptera olfactory receptors revealed by deorphanization of a moth repertoire. *Nature Communications*, *8*, 15709.

EPPO. (2019). EPPO A1 and A2 Lists of pests recommended for regulation as quarantine pests. https://gd.eppo.int/taxon/RHYCFE/documents, PM7/083(1).

Faleiro, J. (2006). A review of the issues and management of the red palm weevil *Rhynchophorus ferrugineus* (Coleoptera: Rhynchophoridae) in coconut and date palm during the last one hundred years. *International Journal of Tropical Insect Science*, *26*(03), 135–154.

Fleischer, J., & Krieger, J. (2018). Insect pheromone receptors–key elements in sensing intraspecific chemical signals. *Frontiers in Cellular Neuroscience*, *12*, 425. https://doi.org/10.3389/fncel.2018.00425

Fleischer, J., & Krieger, J. (2020). Molecular mechanisms of pheromone detection. In G. Blomquist & R. Vogt (Eds.), *Insect Pheromone Biochemistry and Molecular Biology* (pp. 355–413). Academic Press. https://doi.org/10.1016/B978-0-12-819628-1.00012-2

Fleischer, J., Pregitzer, P., Breer, H., & Krieger, J. (2018). Access to the odor world: Olfactory receptors and their role for signal transduction in insects. *Cellular and Molecular Life Sciences*, *75*, 485–508. https://doi.org/10.1007/s00018-017-2627-5

Große-Wilde, E., Gohl, T., Bouché, E., Breer, H., & Krieger, J. (2007). Candidate pheromone receptors provide the basis for the response of distinct antennal neurons to pheromonal compounds. *European Journal of Neuroscience*, *25*(8), 2364–2373.

Große-Wilde, E., Svatoš, A., & Krieger, J. (2006). A pheromone-binding protein mediates the bombykol-induced activation of a pheromone receptor in vitro. *Chemical Senses*, *31*(6), 547–555.

Guarino, S., Bue, P. L., Peri, E., & Colazza, S. (2011). Responses of Rhynchophorus ferrugineus adults to selected synthetic palm esters: Electroantennographic studies and trap catches in an urban environment. *Pest Management Science*, *67*(1), 77–81.

Hammer, Ø., Harper, D. A., & Ryan, P. D. (2001). PAST: Paleontological statistics software package for education and data analysis. *Palaeontologia Electronica*, *4*(1), *9*.

Harini, K., & Sowdhamini, R. (2015). Computational approaches for decoding select odorant-olfactory receptor interactions using mini-virtual screening. *PLoS One*, *10*(7), e0131077.

Jones, P. L., Pask, G. M., Rinker, D. C., & Zwiebel, L. J. (2011). Functional agonism of insect odorant receptor ion channels. *Proceedings of the National Academy of Sciences*, *108*(21), 8821–8825.

Katoh, K., Rozewicki, J., & Yamada, K. D. (2017). MAFFT online service: Multiple sequence alignment, interactive sequence choice and visualization. *Briefings in Bioinformatics*, *20*(4), 1160–1166. https://doi.org/10.1093/bib/bbx108

Kurtovic, A., Widmer, A., & Dickson, B. J. (2007). A single class of olfactory neurons mediates behavioural responses to a Drosophila sex pheromone. *Nature*, *446*(7135), 542.

Larsson, M. C., Domingos, A. I., Jones, W. D., Chiappe, M. E., Amrein, H., & Vosshall, L. B. (2004). Or83b encodes a broadly expressed odorant receptor essential for Drosophila olfaction. *Neuron*, *43*(5), 703–714.

Leal, W. S. (2013). Odorant reception in insects: Roles of receptors, binding proteins, and degrading enzymes. *Annual Review of Entomology*, *58*, 373–391.

Leal, W. S. (2014). Deciphering the Rosetta Stone of insect chemical communication. *American Entomologist*, *60*(4), 223–230.

Leal, W. S. (2017). Reverse chemical ecology at the service of conservation biology. *Proceedings of the National Academy of Sciences*, *114*(46), 12094–12096. https://doi.org/10.1073/pnas.1717375114.

Leal, W. S., Barbosa, R. M. R., Xu, W., Ishida, Y., Syed, Z., Latte, N., Chen, A. M., Morgan, T. I., Cornel, A. J., & Furtado, A. (2008). Reverse and conventional chemical ecology approaches for the development of oviposition attractants for Culex mosquitoes. *PLoS One*, *3*(8), e3045.

Mansourian, S., & Stensmyr, M. C. (2015). The chemical ecology of the fly. *Current Opinion in Neurobiology*, *34*, 95–102.

Meinwald, J., Leal, W. S., & Kubanek, J. (2018). Molecules as biotic messengers. *ACS Omega*, *3*(4), 4048–4053.

Mitchell, R. F., Hughes, D. T., Luetje, C. W., Millar, J. G., Soriano-Agatón, F., Hanks, L. M., & Robertson, H. M. (2012). Sequencing and characterizing odorant receptors of the cerambycid beetle *Megacyllene caryae*. *Insect Biochemistry and Molecular Biology*, *42*(7), 499–505.

Mitchell, R. F., Schneider, T. M., Schwartz, A. M., Andersson, M. N., & McKenna, D. D. (2020). The diversity and evolution of odorant receptors in beetles (Coleoptera). *Insect Molecular Biology*, *29*(1), 77–91.

Montagné, N., de Fouchier, A., Newcomb, R. D., & Jacquin-Joly, E. (2015). Advances in the identification and characterization of olfactory receptors in insects. In R. Glatz (Ed.), *Progress in molecular biology and translational science* (Vol. *130*, pp. 55–80). Elsevier. https://doi.org/10.1016/bs.pmbts.2014.11.003

Nakagawa, T., Sakurai, T., Nishioka, T., & Touhara, K. (2005). Insect sex-pheromone signals mediated by specific combinations of olfactory receptors. *Science*, *307*(5715), 1638–1642.

Oehlschlager, A. C. (2016). Palm weevil pheromones – discovery and use. *Journal of Chemical Ecology*, *42*(7), 617–630. https://doi.org/10.1007/s10886-016-0720-0.

Olsson, S. B., & Hansson, B. S. (2013). Electroantennogram and single sensillum recording in insect antennae. In K. Touhara (Ed.), *Pheromone signaling* (pp. 157–177). Springer. https://doi.org/10.1007/978-1-62703-619-1_11

Perez, A. L., Campos, Y., Chinchilla, C. M., Oehlschlager, A. C., Gries, G., Gries, R., Giblin-Davis, R. M., Castrillo, G., Peña, J. E., Duncan, R. E., Gonzalez, L. M., Pierce Jr., H. D., McDonald, R., & Andrade, R. (1997). Aggregation pheromones and host kairomones of West Indian sugarcane weevil, Metamasius hemipterus sericeus. *Journal of Chemical Ecology*, *23*(4), 869–888.

Peri, E., Rochat, D., Belusic, G., Ilic, M., Soroker, V., Barkan, S., & Colazza, S. (2017). *Rhynchophorus ferrugineus*: Behavior, ecology, and communication. In V. Soroker & S. Colazza (Eds.), *Handbook of major palm pests: Biology and management* (pp. 105–130). Wiley. https://doi.org/10.1002/9781119057468.ch5

Picimbon, J.-F. (2019). Evolution of Protein Physical Structures in Insect Chemosensory Systems. In J.-F. Picimbon (Ed.), *Olfactory concepts of insect control-alternative to insecticides* (231–263). Springer. https://doi.org/10.1007/978-3-030-05165-5_10

Sato, K., Pellegrino, M., Nakagawa, T., Nakagawa, T., Vosshall, L. B., & Touhara, K. (2008). Insect olfactory receptors are heteromeric ligand-gated ion channels. *Nature*, *452*(7190), 1002–1006.

Schmittgen, T. D., & Livak, K. J. (2008). Analyzing real-time PCR data by the comparative CT method. *Nature Protocols*, *3*(6), 1101–1108.

Soffan, A., Antony, B., Abdelazim, M., Shukla, P., Witjaksono, W., Aldosari, S. A., & Aldawood, A. S. (2016). Silencing the Olfactory Co-Receptor RferOrco reduces the response to pheromones in the red palm weevil, Rhynchophorus ferrugineus. *PLOS One*, *11*(9), e0162203. https://doi.org/10.1371/journal.pone.0162203

Stamatakis, A. (2014). RAxML version 8: A tool for phylogenetic analysis and post-analysis of large phylogenies. *Bioinformatics*, *30*(9), 1312–1313.

Syed, Z., Ishida, Y., Taylor, K., Kimbrell, D. A., & Leal, W. S. (2006). Pheromone reception in fruit flies expressing a moth's odorant receptor. *Proceedings of the National Academy of Sciences*, *103*(44), 16538–16543. https://doi.org/10.1073/pnas.0607874103.

Vacas, S., Melita, O., Michaelakis, A., Milonas, P., Minuz, R., Riolo, P., Abbass, M. K., Lo Bue, P., Colazza, S., Peri, E., Soroker, V., Livne, Y., Primo, J., & Navarro-Llopis, V. (2017). Lures for red palm weevil trapping systems: Aggregation pheromone and synthetic kairomone. *Pest Management Science*, *73*(1), 223–231.

Venthur, H., & Zhou, J.-J. (2018). Odorant receptors and odorant-binding proteins as insect pest control targets: A comparative analysis. *Frontiers in Physiology*, *9*, 1163.

Vosshall, L. B., & Hansson, B. S. (2011). A unified nomenclature system for the insect olfactory coreceptor. *Chemical Senses*, *36*(6), 497–498.

Wicher, D., Schäfer, R., Bauernfeind, R., Stensmyr, M. C., Heller, R., Heinemann, S. H., & Hansson, B. S. (2008). Drosophila odorant receptors are both ligand-gated and cyclic-nucleotide-activated cation channels. *Nature*, *452*(7190), 1007–1011.

Yan, H., Jafari, S., Pask, G., Zhou, X., Reinberg, D., & Desplan, C. (2020). Evolution, developmental expression and function of odorant receptors in insects. *Journal of Experimental Biology*, *223*(Suppl 1). https://doi.org/10.1242/jeb.208215

Yuvaraj, J. K., Roberts, R. E., Sonntag, Y., Hou, X.-Q., Grosse-Wilde, E., Machara, A., Zhang, D.-D., Hansson, B. S., Johanson, U., Löfstedt, C., & Andersson, M. N. (2021). Putative ligand binding sites of two functionally characterized bark beetle odorant receptors. *BMC Biology*, *19*(1), 1–21.

SUPPORTING INFORMATION

Additional supporting information may be found online in the Supporting Information section.

How to cite this article: Antony B, Johny J, Montagné N, et al. Pheromone receptor of the globally invasive quarantine pest of the palm tree, the red palm weevil (*Rhynchophorus ferrugineus*). *Mol Ecol*. 2021;30:2025–2039. https://doi.org/10.1111/mec.15874